Networks and Heterogeneous Media

https://www.aimspress.com/journal/nhm

NHM, 21(4): 1426–1449.
DOI: 10.3934/nhm.2026054
Received: 04 May 2026
Revised: 25 June 2026
Accepted: 30 June 2026
Published: 06 July 2026

Research article

Event-triggered non-synchronous stabilization for Markov jump systems

Tianze Chai*

School of Computer Science and Technology, Anhui University of Technology, Ma'anshan 243032, China

* **Correspondence:** Email: tianzechai@ahut.edu.cn.

Abstract: The event-triggered non-synchronous stabilization problem for Markov jump systems was investigated via state-feedback control. The possible mismatch between the plant and controller modes was modeled by a hidden Markov model. Both memoryless and memory-based switched event-triggered mechanisms were proposed to reduce the frequency of controller updates. Two sufficient conditions were established to guarantee the stochastic stability of the closed-loop system by employing Lyapunov–Krasovskii functionals, free-weighting matrices, and stochastic analysis. Computationally tractable schemes were then developed to obtain the state-feedback controller gains via congruence transformations. A numerical example is presented to illustrate the efficiency of the switched event-triggered non-synchronous state-feedback control schemes.

Keywords: Markov jump system; switched event-triggered mechanism; stochastic stability; non-synchronous control; state-feedback control

1. Introduction

Markov jump systems (MJSs), characterized by discrete modes governed by probabilistic transition laws, provide a robust framework for modeling systems subject to abrupt structural or environmental variations. By capturing stochastic switching behavior, MJSs have found extensive application in fields such as power systems, cyber-physical systems, robotics, automated manufacturing, aerospace engineering, and large-scale economic systems. In these contexts, sudden operational changes stemming from component failures, subsystem reconfigurations, or environmental disturbances are naturally described by Markovian switching processes. With the rapid evolution of communication technologies, the analysis and synthesis of MJSs within networked control frameworks have been extensively investigated from several perspectives, including communication protocols [1, 2], cyber attacks and security constraints [3–5], and sampled-data sliding-mode control with mixed delays and Lévy noises [6].

In networked Markov jump control systems, communication resources are inherently limited. Potential mismatches may arise between the modes of the plant and the controller due to network-induced issues such as network congestion, data loss, packet reordering, and quantization errors. Compared with synchronous control, non-synchronous control offers a more suitable approach for handling such challenges. This has been explored in several studies. For instance, Tao and Wu [7] investigated non-synchronous stabilization for linear MJSs under complex transition probabilities, deriving sufficient conditions in terms of the original system matrices that ensure regularity, causality, and stochastic stability. Zhou et al. [8] considered discrete-time fuzzy MJSs involving dynamic quantization and developed a non-synchronous dissipative control scheme alongside a two-step iterative approach to optimize the dissipativity level and determine control parameters. More recently, Wang et al. [9] developed non-synchronous stabilization conditions formulated in terms of linear matrix inequalities (LMIs) for discrete-time singular MJSs under partially known probabilistic information.

To optimize the use of limited communication resources, event-triggered mechanisms (ETMs) have been introduced to networked Markov jump control systems. Unlike conventional sampled-data mechanisms [10], ETMs update control inputs only when pre-specified triggering conditions are violated, thereby significantly reducing redundant data transmission [11–13]. Given that the frequency of triggering events directly dictates the communication load and the degree of resource consumption, extensive research has been devoted to developing efficient ETMs for MJSs, including the self-triggered mechanism [14], periodic ETM [15], dynamic ETM [16], two-channel ETM [17], and switched ETMs (SETMs) [18, 19]. Among them, the SETM switches between the waiting interval and the event-detection interval, so that it can maintain a lower triggering frequency and achieve a more favorable balance between implementation complexity and communication efficiency than other ETMs [20–22]. It is important to note that the SETMs considered for MJSs in the existing literature are memoryless, meaning that they do not retain past state information. This opens up possibilities for further investigation into more sophisticated triggering strategies.

Building on the above observations, this paper investigates the event-triggered non-synchronous stabilization problem for MJSs under network-induced mode mismatches. The main innovations and contributions of this paper can be summarized as follows:

1) By modeling the mode mismatches via a hidden Markov model (HMM), the non-synchronous stabilization problem for MJSs is addressed under two distinct SETMs: A memoryless SETM and a memory-based SETM. In contrast to existing SETM studies for MJSs (e.g., [18, 19]), the proposed memory-based SETM introduces a memory term based on the averaged historical state into the triggering condition.

2) Non-synchronous stochastic stability criteria and state-feedback controller synthesis schemes are derived for both SETMs by using Lyapunov–Krasovskii functionals (LKFs), free-weighting matrices, conditional expectation and several matrix inequalities. Numerical results demonstrate that the proposed non-synchronous control schemes can guarantee convergence of the closed-loop system states and achieve fewer triggering events than the schemes in [23, 24].

The remainder of this paper is organized as follows: Section 2 presents the system formulation, including the Markov jump model, the state-feedback controller, and memoryless as well as memory-based SETMs. Section 3 develops the main theoretical schemes, including stochastic stability analysis and the controller design conditions, together with their detailed proofs. Section 4 provides a multiple-mode VTOL helicopter example to verify the effectiveness of the proposed theorems. Finally, Section 5 concludes the paper.

Notations: We use the notation $\mathbb{E}\{\cdot\}$ to stand for mathematical expectation. The symbol $\Pr\{\cdot\}$ denotes probability. The notation $\mathrm{diag}\{\cdot\}$ refers to a block-diagonal matrix formed by its arguments. The notation $\mathbb{R}^n$ denotes the n-dimensional Euclidean space, and $\mathbb{R}^{n\times m}$ represents the set of all $n \times m$ real matrices. The symbol I denotes the identity matrix of appropriate dimension. For a matrix Z, $\mathrm{He}\{Z\}$ denotes $Z+Z^\top$. The notation $\|\cdot\|$ represents the Euclidean norm. The notation $\mathrm{col}\{\cdot\}$ denotes the column vector formed by its arguments, and the symbol $*$ denotes the symmetric term in a symmetric block matrix. In addition, matrix inequalities are interpreted in the symmetric sense whenever dimensions are appropriate.

2. Preliminaries

Consider the MJS

$$\dot{x}(t) = A_{r(t)}x(t) + B_{r(t)}u(t), \tag{2.1}$$

where $x(t) \in \mathbb{R}^n$ is the state and $u(t) \in \mathbb{R}^p$ is the control input. The system mode $r(t)$ is a continuous-time Markov process taking values in $\mathcal{N} = \{1, 2, \ldots, N\}$ with generator $\Pi = [\pi_{ij}]$. Its transition law is given by

$$\Pr\{r(t+\ell) = j \,|\, r(t) = i\} = \begin{cases} \pi_{ij}\ell + o(\ell), & i \neq j, \\ 1 + \pi_{ii}\ell + o(\ell), & i = j, \end{cases}$$

where $\ell > 0$, $\lim_{\ell\to 0^+} \frac{o(\ell)}{\ell} = 0$, $\pi_{ij} \geq 0$ for $i, j \in \mathcal{N}$ with $i \neq j$, and $\sum\limits_{j=1}^{N} \pi_{ij} = 0$ [25].

In this paper, two SETMs are considered to reduce the number of triggering events, namely a memoryless SETM and a memory-based SETM. For both SETMs, after each measurement transmission, the event-triggered condition is not monitored until a minimum waiting period has elapsed, after which a new measurement value is transmitted to the controller once the condition is violated. First, as in [26], the memoryless SETM is introduced as

$$t_{k+1} = \min\left\{ t \geq t_k + h \,\middle|\, e_k^\top(t)\Omega_i e_k(t) \geq \beta x^\top(t)\Omega_i x(t) \right\}, \tag{2.2}$$

where t_k and t_{k+1} denote the kth and $(k+1)$th triggering instants, respectively, with $t_0 = 0$. Moreover, $e_k(t) \triangleq x(t) - x(t_k)$ denotes the deviation of the current state from the most recently transmitted state. The matrix $\Omega_i > 0$ is the mode-dependent weighting matrix, and $\beta > 0$ is the prescribed triggering threshold. $h > 0$ is the prescribed minimum waiting time between two consecutive triggering events.

Remark 1. The minimum waiting time h in the proposed SETM is introduced to exclude Zeno behavior in a direct way. Since each triggering instant satisfies $t_{k+1} - t_k \geq h > 0$, a strictly positive lower bound on the inter-event interval is guaranteed. This design is simple and easy to implement because the triggering condition is not continuously checked during the waiting interval $[t_k, t_k + h)$. The influence of h on the triggering performance is further examined in Table 3.

The memory-based SETM is given by

$$t_{k+1} = \min\left\{ t \geq t_k + h \,\middle|\, e_k^\top(t)\Omega_i e_k(t) \geq \beta\left(x^\top(t)\Omega_i x(t) + \left(\frac{1}{\delta t}\int_{t-\delta t}^{t} x(s)\,\mathrm{d}s\right)^\top \Omega_i \left(\frac{1}{\delta t}\int_{t-\delta_t}^{t} x(s)\,\mathrm{d}s\right)\right)\right\}, \tag{2.3}$$

where $\delta t > 0$. Here, the memory term $(\frac{1}{\delta t}\int_{t-\delta t}^{t} x(s)\,\mathrm{d}s)^{\top}\Omega_i(\frac{1}{\delta t}\int_{t-\delta t}^{t} x(s)\,\mathrm{d}s)$ is generated from the averaged historical state information $\frac{1}{\delta t}\int_{t-\delta t}^{t} x(s)\,\mathrm{d}s$, which denotes the short-time average of the system state over the interval $[t-\delta t, t]$. In this way, the triggering decision depends not only on the instantaneous state energy but also on the recent state evolution accumulated through $\frac{1}{\delta t}\int_{t-\delta t}^{t} x(s)\,\mathrm{d}s$.

Remark 2. The averaged historical state $\frac{1}{\delta t}\int_{t-\delta t}^{t} x(s)\mathrm{d}s$ in the memory-based SETM can be interpreted from a frequency-domain perspective. Specifically, $\frac{1}{\delta t}\int_{t-\delta t}^{t} x(s)\mathrm{d}s$ acts as a low-pass filter applied to $x(t)$, with the magnitude response $\left|\frac{\sin(\omega\delta t/2)}{\omega\delta t/2}\right|$. This filtering effect attenuates high-frequency components of the state signal, thereby reducing the sensitivity of the triggering condition to rapid state fluctuations. By mitigating the effects of such fluctuations, the attenuation of high-frequency components may help maintain closed-loop system stability under the proposed stability criterion.

Similar to the approach used in [27, 28], the control input $u(t)$ is designed based on state feedback. The control law in this paper is defined as

$$u(t) = K_{s(t)}x(t_k),\ t \in [t_k, t_{k+1}), \tag{2.4}$$

where $K_{s(t)}$ denotes the feedback gain associated with the controller mode $s(t)$. Here, $s(t)$ ($s(t) \in \mathcal{M} = \{1, 2, \ldots, M\}$) is a stochastic variable acting as a detector for acquiring the switching information of the MJS. Moreover, the stochastic relationship between the system mode $r(t)$ and the controller mode $s(t)$ is characterized by the conditional probability matrix $\Phi = [\phi_{im}]$ with

$$\Pr\{s(t) = m \mid r(t) = i\} = \phi_{im},$$

in which $0 \le \phi_{im} \le 1$ and $\sum_{m=1}^{M} \phi_{im} = 1$. Consequently, the plant and controller modes form a HMM.

Let $\tau(t) = t - t_k$ denote the elapsed time since the latest triggering instant, so that $x(t_k) = x(t - \tau(t))$. Substituting Eq (2.4) into Eq (2.1), one obtains the state-feedback closed-loop system

$$\dot{x}(t) = \begin{cases} A_{r(t)}x(t) + B_{r(t)}K_{s(t)}x(t-\tau(t)), & t \in [t_k, t_k + h), \\ (A_{r(t)} + B_{r(t)}K_{s(t)})x(t) - B_{r(t)}K_{s(t)}e_k(t), & t \in [t_k + h, t_{k+1}). \end{cases} \tag{2.5}$$

The purpose of this paper is to achieve stochastic stabilization of the system in Eq (2.1) with controller Eq (2.4) under the memoryless SETM in Eq (2.2) and the memory-based SETM in Eq (2.3). The following definitions and lemma are needed.

Definition 1 (Weak infinitesimal operator)**.** [29] The weak infinitesimal operator of the stochastic process $\{(x(t), r(t))\}_{t\ge 0}$ is given as

$$\mathcal{L}V(x(t), t, r(t)) = \lim_{\Delta\to 0^+} \frac{1}{\Delta}\left[\mathbb{E}\{V(x(t+\Delta), t+\Delta, r(t+\Delta)) \,\big|\, x(t), t, r(t) = i\} - V(x(t), t, r(t))\right].$$

Definition 2 (Stochastic stability)**.** [30] The system is said to be stochastically stable if, for any initial condition $x(0) = x_0$ and $r(0) = r_0$,

$$\int_0^\infty \mathbb{E}\left\{\|x(t)\|^2 \,\big|\, x_0, r_0\right\}\mathrm{d}t < \infty$$

holds true.

Lemma 1 (Jensen's inequality)**.** [31] *Let $U \in \mathbb{R}^{n\times n}$ be a positive definite matrix, and let $\varepsilon : [p, q] \to \mathbb{R}^n$ be a vector function. Then, the following inequality holds:*

$$\left[\int_p^q \varepsilon(\sigma)\,\mathrm{d}\sigma\right]^\top U \left[\int_p^q \varepsilon(\sigma)\,\mathrm{d}\sigma\right] \leq (q-p)\int_p^q \varepsilon^\top(\sigma)\,U\,\varepsilon(\sigma)\,\mathrm{d}\sigma.$$

3. Main results

3.1. Analysis and controller design under the memoryless scheme

This subsection concerns the state-feedback closed-loop system in Eq (2.5) under the memoryless SETM in Eq (2.2). We can establish an analysis result regarding the stochastic stability as follows:

Theorem 1. *Given feedback gains K_m ($m = 1, \dots, M$) and a scalar $\beta > 0$, the closed-loop system in Eq (2.5) is stochastically stable if there exist matrices $S \succ 0$, $P_i \succ 0$, $\Omega_i \succ 0$ ($i = 1, \dots, N$), and a free-weighting matrix Q satisfying*

$$\Lambda_{1i} = \begin{bmatrix} \Theta_{11}^{(1)} & \Theta_{12}^{(1)} & \Theta_{13}^{(1)} \\ * & -\mathrm{He}(Q) & \Theta_{23}^{(1)} \\ * & * & -S \end{bmatrix} \prec 0, \tag{3.1}$$

$$\Lambda_{2i} = \begin{bmatrix} \Theta_{11}^{(2)} & \Theta_{12}^{(2)} & \Theta_{13}^{(2)} \\ * & -\mathrm{He}(Q) & \Theta_{23}^{(2)} \\ * & * & -\Omega_i \end{bmatrix} \prec 0, \tag{3.2}$$

where

$$\begin{aligned}
\Theta_{11}^{(1)} &= \mathrm{He}(Q^\top A_i) + \sum_{j=1}^{N} \pi_{ij} P_j, \\
\Theta_{12}^{(1)} &= P_i - Q^\top + A_i^\top Q, \\
\Theta_{13}^{(1)} &= Q^\top B_i \sum_{m=1}^{M} \phi_{im} K_m, \\
\Theta_{23}^{(1)} &= Q^\top B_i \sum_{m=1}^{M} \phi_{im} K_m, \\
\Theta_{11}^{(2)} &= \beta\Omega_i + \mathrm{He}(Q^\top A_i) + \mathrm{He}\left(Q^\top B_i \sum_{m=1}^{M} \phi_{im} K_m\right) + \sum_{j=1}^{N} \pi_{ij} P_j, \\
\Theta_{12}^{(2)} &= P_i - Q^\top + A_i^\top Q + \left(\sum_{m=1}^{M} \phi_{im} K_m\right)^\top B_i^\top Q, \\
\Theta_{13}^{(2)} &= -Q^\top B_i \sum_{m=1}^{M} \phi_{im} K_m, \\
\Theta_{23}^{(2)} &= -Q^\top B_i \sum_{m=1}^{M} \phi_{im} K_m.
\end{aligned}$$

Proof. Consider the following piecewise LKF:

$$V(x(t),t,r(t)) = \begin{cases} V_1(x(t),t,r(t)) + V_2(x(t),t), & t \in [t_k, t_k+h), \\ V_1(x(t),t,r(t)), & t \in [t_k+h, t_{k+1}), \end{cases}$$

where

$$V_1(x(t),t,r(t)) = x^\top(t)P_{r(t)}x(t),$$
$$V_2(x(t),t) = (h-\tau(t))x^\top(t-\tau(t))Sx(t-\tau(t)).$$

Using Definition 1, one has

$$\begin{aligned}
\mathcal{L}V_1(x(t),t,r(t)) &= \lim_{\Delta\to 0^+}\frac{1}{\Delta}\left[\mathbb{E}\{x^\top(t+\Delta)P_{r(t+\Delta)}x(t+\Delta)\,\big|\,x(t),t,r(t)=i\} - x^\top(t)P_{r(t)}x(t)\right] \\
&= \lim_{\Delta\to 0^+}\frac{1}{\Delta}\left[\sum_{j=1}^{N}\Pr\{r(t+\Delta)=j\mid r(t)=i\}x^\top(t+\Delta)P_jx(t+\Delta) - x^\top(t)P_ix(t)\right] \\
&= \sum_{j=1}^{N}\pi_{ij}x^\top(t)P_jx(t) + \lim_{\Delta\to 0^+}\frac{x^\top(t+\Delta)P_ix(t+\Delta)-x^\top(t)P_ix(t)}{\Delta} \\
&= 2x^\top(t)P_i\dot{x}(t) + x^\top(t)\left(\sum_{j=1}^{N}\pi_{ij}P_j\right)x(t), \\
\mathcal{L}V_2(x(t),t) &= -x^\top(t-\tau(t))Sx(t-\tau(t)).
\end{aligned}$$

Next, the proof consists of three parts.

Part I: In the waiting interval, i.e., $t \in [t_k, t_k+h)$.

In this interval,

$$\mathcal{L}V(x(t),t,r(t)) = 2x^\top(t)P_i\dot{x}(t) + x^\top(t)\Big(\sum_{j=1}^{N}\pi_{ij}P_j\Big)x(t) - x^\top(t-\tau(t))Sx(t-\tau(t)). \tag{3.3}$$

Since the controller mode $s(t)$ may differ from the system mode $r(t)$, the feedback gain $K_{s(t)}$ is still random when $r(t)=i$. Taking the conditional expectation of the system in Eq (2.5) with respect to $s(t)$ under $r(t)=i$, and using $\Pr\{s(t)=m\mid r(t)=i\}=\phi_{im}$, one obtains

$$\begin{aligned}
0 &= \mathbb{E}\{-\dot{x}(t) + A_{r(t)}x(t) + B_{r(t)}K_{s(t)}x(t-\tau(t))\mid r(t)=i\} \\
&= \sum_{m=1}^{M}\Pr\{s(t)=m\mid r(t)=i\}\{-\dot{x}(t)+A_ix(t)+B_iK_mx(t-\tau(t))\} \\
&= -\dot{x}(t) + A_ix(t) + \sum_{m=1}^{M}\phi_{im}B_iK_mx(t-\tau(t)),
\end{aligned}$$

from which we can establish the following free-weighting matrix equality:

$$0 = 2\left[\dot{x}^\top(t) + x^\top(t)\right]\cdot Q^\top\cdot\left[-\dot{x}(t)+A_ix(t)+\sum_{m=1}^{M}\phi_{im}B_iK_mx(t-\tau(t))\right]. \tag{3.4}$$

Let $\eta_1(t) = \mathrm{col}\{x(t), \dot{x}(t), x(t-\tau(t))\}$. Then, by combining Eqs (3.3) and (3.4), one obtains

$$\begin{aligned}\mathbb{E}\{\mathcal{L}V(x(t),t,r(t))\} &= \mathbb{E}\Big\{\mathcal{L}V(x(t),t,r(t)) + 2[\dot{x}^\top(t) + x^\top(t)]\cdot Q^\top \cdot \Big[-\dot{x}(t)+A_i x(t)+\sum_{m=1}^{M}\phi_{im}B_iK_m x(t-\tau(t))\Big]\Big\} \\ &= \mathbb{E}\{\,\eta_1^\top(t)\Lambda_{1i}\eta_1(t)\,\}\,. \end{aligned} \tag{3.5}$$

Since Eq (3.1) guarantees that $\Lambda_{1i} \prec 0$ for $i \in \{1,2,\dots,N\}$, there exists a scalar $\sigma_1 > 0$ such that $\Lambda_{1i} \preceq -\sigma_1 I$, which implies $\eta_1^\top(t)\Lambda_{1i}\eta_1(t) \le -\sigma_1\|\eta_1(t)\|^2 \le -\sigma_1\|x(t)\|^2$. Therefore, it follows from Eq (3.5) that

$$\mathbb{E}\{\mathcal{L}V(x(t),t,r(t))\} \le -\sigma_1\mathbb{E}\Big\{\|x(t)\|^2\Big\}\,. \tag{3.6}$$

Part II: In the event-detection interval, i.e., $t \in [t_k + h, t_{k+1})$.

In this interval,

$$\mathcal{L}V(x(t),t,r(t)) = 2x^\top(t)P_i\dot{x}(t) + x^\top(t)\Big(\sum_{j=1}^{N}\pi_{ij}P_j\Big)x(t). \tag{3.7}$$

As in Part I, taking the conditional expectation of the system in Eq (2.5) with respect to $s(t)$ under $r(t) = i$ gives

$$0 = -\dot{x}(t) + \Big(A_i + \sum_{m=1}^{M}\phi_{im}B_iK_m\Big)x(t) - \sum_{m=1}^{M}\phi_{im}B_iK_m e_k(t),$$

from which we can establish the following free-weighting matrix equality:

$$0 = 2\Big[\dot{x}^\top(t) + x^\top(t)\Big]\cdot Q^\top \cdot \Big[-\dot{x}(t) + \Big(A_i + \sum_{m=1}^{M}\phi_{im}B_iK_m\Big)x(t) - \sum_{m=1}^{M}\phi_{im}B_iK_m e_k(t)\Big]. \tag{3.8}$$

During $t \in [t_k+h, t_{k+1})$, no new event has been generated before t_{k+1}. Hence, the triggering condition in the memoryless SETM in Eq (2.2) has not yet been satisfied, which implies

$$0 \le x^\top(t)\beta\Omega_i x(t) - e_k^\top(t)\Omega_i e_k(t). \tag{3.9}$$

Let $\eta_2(t) = \mathrm{col}\{x(t), \dot{x}(t), e_k(t)\}$. Then, by combining Eqs (3.7)–(3.9), one obtains

$$\begin{aligned}\mathbb{E}\{\mathcal{L}V(x(t),t,r(t))\} \le \mathbb{E}\Big\{ & \mathcal{L}V(x(t),t,r(t)) + 2[\dot{x}^\top(t) + x^\top(t)]\cdot Q^\top \cdot \\ & \Big[-\dot{x}(t) + \Big(A_i + \sum_{m=1}^{M}\phi_{im}B_iK_m\Big)x(t) - \sum_{m=1}^{M}\phi_{im}B_iK_m e_k(t)\Big] \\ & + x^\top(t)\beta\Omega_i x(t) - e_k^\top(t)\Omega_i e_k(t)\Big\} \\ = \mathbb{E}\{ & \eta_2^\top(t)\Lambda_{2i}\eta_2(t)\}\,. \end{aligned} \tag{3.10}$$

Since Eq (3.2) guarantees that $\Lambda_{2i} \prec 0$ for $i \in \{1,2,\dots,N\}$, there exists a scalar $\sigma_2 > 0$ such that $\Lambda_{2i} \preceq -\sigma_2 I$, which implies $\eta_2^\top(t)\Lambda_{2i}\eta_2(t) \le -\sigma_2\|\eta_2(t)\|^2 \le -\sigma_2\|x(t)\|^2$. Therefore, it follows from Eq (3.10) that

$$\mathbb{E}\{\mathcal{L}V(x(t),t,r(t))\} \leq -\sigma_2\mathbb{E}\Big\{\|x(t)\|^2\Big\}. \tag{3.11}$$

Part III: Synthesis.

Combining Eqs (3.6) and (3.11), and taking $\sigma = \min\{\sigma_1, \sigma_2\} > 0$, it follows that, for all $t \geq 0$,

$$\mathbb{E}\{\mathcal{L}V(x(t),t,r(t))\} \leq -\sigma\mathbb{E}\Big\{\|x(t)\|^2\Big\}. \tag{3.12}$$

For any $t^\star > 0$, using Dynkin's formula and Eq (3.12) yields

$$\mathbb{E}\{V(x(t^\star),t^\star,r(t^\star))\} - V(x(0),0,r(0)) = \int_0^{t^\star} \mathbb{E}\{\mathcal{L}V(x(t),t,r(t))\}\,\mathrm{d}t \leq -\sigma\int_0^{t^\star} \mathbb{E}\Big\{\|x(t)\|^2\Big\}\,\mathrm{d}t. \tag{3.13}$$

Taking the limit as $t^\star \to \infty$ in Eq (3.13), and noting that $\mathbb{E}\{V(x(t^\star),t^\star,r(t^\star))\} \geq 0$, one obtains

$$\int_0^\infty \mathbb{E}\Big\{\|x(t)\|^2\Big\}\,\mathrm{d}t \leq \frac{1}{\sigma}V(x(0),0,r(0)) < \infty.$$

According to Definition 2, the system in Eq (2.5) is stochastically stable. The proof is complete.

Remark 3. Representative ETM-based studies on MJSs, such as [15–17], employ direct or periodic event-triggering rules. Meanwhile, SETMs have been developed in [18,21], but the mismatch between the plant and controller modes was not considered. By contrast, Theorem 1 employs the memoryless SETM in Eq (2.2), which switches between a waiting interval and an event-detection interval, and further embeds it into a non-synchronous HMM framework, where the conditional probabilities ϕ_{im} are explicitly involved in the stability criterion.

Theorem 2. *Given a scalar $\beta > 0$, if there exist matrices $\bar{P}_i \succ 0$, $\bar{\Omega}_i \succ 0$ $(i = 1,\dots,N)$, $\bar{S} \succ 0$, an invertible matrix $\bar{Q}$, and general matrices $\bar{K}_m$ $(m = 1,\dots,M)$ satisfying the following LMIs:*

$$\bar{\Lambda}_{1i} = \begin{bmatrix} \bar{\Theta}_{11}^{(1)} & \bar{\Theta}_{12}^{(1)} & \bar{\Theta}_{13}^{(1)} \\ * & -\mathrm{He}(\bar{Q}) & \bar{\Theta}_{23}^{(1)} \\ * & * & -\bar{S} \end{bmatrix} \prec 0, \tag{3.14}$$

$$\bar{\Lambda}_{2i} = \begin{bmatrix} \bar{\Theta}_{11}^{(2)} & \bar{\Theta}_{12}^{(2)} & \bar{\Theta}_{13}^{(2)} \\ * & -\mathrm{He}(\bar{Q}) & \bar{\Theta}_{23}^{(2)} \\ * & * & -\bar{\Omega}_i \end{bmatrix} \prec 0, \tag{3.15}$$

where

$$\bar{\Theta}_{11}^{(1)} = \mathrm{He}(A_i\bar{Q}) + \sum_{j=1}^{N}\pi_{ij}\bar{P}_j,$$

$$\bar{\Theta}_{12}^{(1)} = \bar{P}_i - \bar{Q} + \bar{Q}^\top A_i^\top,$$

$$\bar{\Theta}_{13}^{(1)} = B_i\sum_{m=1}^{M}\phi_{im}\bar{K}_m,$$

$$\bar{\Theta}_{23}^{(1)} = B_i \sum_{m=1}^{M} \phi_{im} \bar{K}_m,$$

$$\bar{\Theta}_{11}^{(2)} = \beta \bar{\Omega}_i + \mathrm{He}(A_i \bar{Q}) + \mathrm{He}\left(B_i \sum_{m=1}^{M} \phi_{im} \bar{K}_m \right) + \sum_{j=1}^{N} \pi_{ij} \bar{P}_j,$$

$$\bar{\Theta}_{12}^{(2)} = \bar{P}_i - \bar{Q} + \bar{Q}^\top A_i^\top + \left(\sum_{m=1}^{M} \phi_{im} \bar{K}_m \right)^\top B_i^\top,$$

$$\bar{\Theta}_{13}^{(2)} = -B_i \sum_{m=1}^{M} \phi_{im} \bar{K}_m,$$

$$\bar{\Theta}_{23}^{(2)} = -B_i \sum_{m=1}^{M} \phi_{im} \bar{K}_m,$$

then the state-feedback controller Eq (2.4) *with gain*

$$K_m = \bar{K}_m \bar{Q}^{-1},\ m \in \mathcal{M}$$

is able to achieve non-synchronous stabilization of the system in Eq (2.5).

Proof. Set

$$P_i = (\bar{Q}^{-1})^\top \bar{P}_i \bar{Q}^{-1}, \quad \Omega_i = (\bar{Q}^{-1})^\top \bar{\Omega}_i \bar{Q}^{-1}, \quad S = (\bar{Q}^{-1})^\top \bar{S} \bar{Q}^{-1}, \quad Q = \bar{Q}^{-1},$$

and define

$$\mathcal{G} = \mathrm{diag}\left\{ (\bar{Q}^{-1})^\top, (\bar{Q}^{-1})^\top, (\bar{Q}^{-1})^\top \right\}.$$

Then, applying the transformation $\mathcal{G}(\cdot)\mathcal{G}^\top$ to the two inequalities $\bar{\Lambda}_{1i} \prec 0$ and $\bar{\Lambda}_{2i} \prec 0$, namely Eqs (3.14) and (3.15), gives

$$\mathcal{G}\bar{\Lambda}_{1i}\mathcal{G}^\top \prec 0,\ \mathcal{G}\bar{\Lambda}_{2i}\mathcal{G}^\top \prec 0.$$

By this congruence transformation, the inequalities (3.1) and (3.2) are obtained. Therefore, the feasibility of Eqs (3.14) and (3.15) implies the feasibility of Eqs (3.1) and (3.2). Thus, the proof is complete.

3.2. Extension to the memory-based scheme

This subsection concerns the state-feedback closed-loop system in Eq (2.5) under the memory-based SETM in Eq (2.3).

Compared with the memoryless scheme, the memory-based analysis involves an additional memory term, which necessitates the introduction of an additional LKF. This functional is embedded into the weak infinitesimal operator analysis to quantify the effect of the memory segment. Moreover, the coupling between the memory variable $\frac{1}{\delta t}\int_{t-\delta t}^{t} x(s)\,\mathrm{d}s$ and other augmented state variables is intricate. To address this complexity, we use more involved free-weighting matrix equalities with richer coupling relations among the memory variable and other augmented state variables to establish explicit cross-term relations among these variables, thereby helping to reduce the conservatism of the derived stability criterion.

Theorem 3. *Given feedback gains K_m ($m = 1, \dots, M$), scalars $\beta > 0$ and $\delta t > 0$, the closed-loop system in Eq (2.5) is stochastically stable if there exist matrices $R > 0$, $S > 0$, $P_i > 0$, $\Omega_i > 0$ ($i = 1, \dots, N$), and a free-weighting matrix Q satisfying*

$$\Gamma_{1i} = \begin{bmatrix} \Xi_{11}^{(1)} & \Xi_{12}^{(1)} & \Xi_{13}^{(1)} & \Xi_{14}^{(1)} \\ * & -\operatorname{He}(Q) & \Xi_{23}^{(1)} & -Q \\ * & * & -S & \Xi_{34}^{(1)} \\ * & * & * & -\delta t R \end{bmatrix} \prec 0, \tag{3.16}$$

$$\Gamma_{2i} = \begin{bmatrix} \Xi_{11}^{(2)} & \Xi_{12}^{(2)} & \Xi_{13}^{(2)} & \Xi_{14}^{(2)} \\ * & -\operatorname{He}(Q) & \Xi_{23}^{(2)} & -Q \\ * & * & -\Omega_i & \Xi_{34}^{(2)} \\ * & * & * & \beta\Omega_i - \delta t R \end{bmatrix} \prec 0, \tag{3.17}$$

where

$$\begin{aligned}
\Xi_{11}^{(1)} &= \delta t R + \operatorname{He}(Q^\top A_i) + \sum_{j=1}^{N} \pi_{ij} P_j, \\
\Xi_{12}^{(1)} &= P_i - Q^\top + A_i^\top Q, \\
\Xi_{13}^{(1)} &= Q^\top B_i \sum_{m=1}^{M} \phi_{im} K_m, \\
\Xi_{14}^{(1)} &= A_i^\top Q, \\
\Xi_{23}^{(1)} &= Q^\top B_i \sum_{m=1}^{M} \phi_{im} K_m, \\
\Xi_{34}^{(1)} &= \left(\sum_{m=1}^{M} \phi_{im} K_m \right)^\top B_i^\top Q, \\
\Xi_{11}^{(2)} &= \delta t R + \beta\Omega_i + \operatorname{He}(Q^\top A_i) + \operatorname{He}\left(Q^\top B_i \sum_{m=1}^{M} \phi_{im} K_m \right) + \sum_{j=1}^{N} \pi_{ij} P_j, \\
\Xi_{12}^{(2)} &= P_i - Q^\top + A_i^\top Q + \left(\sum_{m=1}^{M} \phi_{im} K_m \right)^\top B_i^\top Q, \\
\Xi_{13}^{(2)} &= -Q^\top B_i \sum_{m=1}^{M} \phi_{im} K_m, \\
\Xi_{14}^{(2)} &= A_i^\top Q + \left(\sum_{m=1}^{M} \phi_{im} K_m \right)^\top B_i^\top Q, \\
\Xi_{23}^{(2)} &= -Q^\top B_i \sum_{m=1}^{M} \phi_{im} K_m, \\
\Xi_{34}^{(2)} &= -\left(\sum_{m=1}^{M} \phi_{im} K_m \right)^\top B_i^\top Q.
\end{aligned}$$

Proof. Consider the following piecewise LKF:

$$V(x(t),t,r(t)) = \begin{cases} V_1(x(t),t,r(t)) + V_2(x(t),t) + V_3(x(t),t), & t \in [t_k, t_k+h), \\ V_1(x(t),t,r(t)) + V_3(x(t),t), & t \in [t_k+h, t_{k+1}). \end{cases}$$

Here,

$$\begin{aligned} V_1(x(t),t,r(t)) &= x^\top(t)P_{r(t)}x(t), \\ V_2(x(t),t) &= (h-\tau(t))x^\top(t-\tau(t))S\,x(t-\tau(t)), \\ V_3(x(t),t) &= \int_{t-\delta t}^{t}(s-t+\delta t)x^\top(s)Rx(s)\,\mathrm{d}s. \end{aligned}$$

Using Definition 1, one obtains

$$\begin{aligned} \mathcal{L}V_1(x(t),t,r(t)) &= 2x^\top(t)P_i\dot{x}(t) + x^\top(t)\Big(\sum_{j=1}^{N}\pi_{ij}P_j\Big)x(t), \\ \mathcal{L}V_2(x(t),t) &= -x^\top(t-\tau(t))S\,x(t-\tau(t)), \\ \mathcal{L}V_3(x(t),t) &= \delta t\,x^\top(t)Rx(t) - \int_{t-\delta t}^{t}x^\top(s)Rx(s)\,\mathrm{d}s. \end{aligned}$$

From Lemma 1, we can conclude

$$\int_{t-\delta t}^{t}x^\top(s)Rx(s)\,\mathrm{d}s \geq \left(\frac{1}{\delta t}\int_{t-\delta t}^{t}x(s)\,\mathrm{d}s\right)^\top \delta tR\left(\frac{1}{\delta t}\int_{t-\delta t}^{t}x(s)\,\mathrm{d}s\right).$$

Therefore,

$$\mathcal{L}V_3(x(t),t) \leq x^\top(t)\delta tRx(t) - \left(\frac{1}{\delta t}\int_{t-\delta t}^{t}x(s)\,\mathrm{d}s\right)^\top \delta tR\left(\frac{1}{\delta t}\int_{t-\delta t}^{t}x(s)\,\mathrm{d}s\right).$$

Next, the proof consists of three parts.

Part I: In the waiting interval, i.e., $t \in [t_k, t_k+h)$.

In this interval,

$$\begin{aligned} \mathcal{L}V(x(t),t,r(t)) \leq{}& 2x^\top(t)P_i\dot{x}(t) + x^\top(t)\Big(\sum_{j=1}^{N}\pi_{ij}P_j\Big)x(t) + x^\top(t)\delta t\,Rx(t) \\ &-\left(\frac{1}{\delta t}\int_{t-\delta t}^{t}x(s)\,\mathrm{d}s\right)^\top \delta t\,R\left(\frac{1}{\delta t}\int_{t-\delta t}^{t}x(s)\,\mathrm{d}s\right) - x^\top(t-\tau(t))S\,x(t-\tau(t)). \end{aligned} \tag{3.18}$$

Following the derivation of Eq (3.4) in Theorem 1, we extend the free-weighting matrix equality to incorporate the averaged historical state term as follows:

$$0 = 2\left[\dot{x}^\top(t) + x^\top(t) + \left(\frac{1}{\delta t}\int_{t-\delta t}^{t}x(s)\,\mathrm{d}s\right)^\top\right]\cdot Q^\top\cdot\left[-\dot{x}(t) + A_ix(t) + \sum_{m=1}^{M}\phi_{im}B_iK_mx(t-\tau(t))\right]. \tag{3.19}$$

Let $\nu_1(t) = \operatorname{col}\left\{x(t), \dot{x}(t), x(t-\tau(t)), \frac{1}{\delta t}\int_{t-\delta t}^{t} x(s)\,\mathrm{d}s\right\}$. Then, by combining Eqs (3.18) and (3.19), one obtains

$$\begin{aligned}
\mathbb{E}\{\mathcal{L}V(x(t),t,r(t))\} &= \mathbb{E}\Bigg\{\mathcal{L}V(x(t),t,r(t)) + 2\Bigg[\dot{x}^\top(t) + x^\top(t) + \left(\frac{1}{\delta t}\int_{t-\delta t}^{t} x(s)\,\mathrm{d}s\right)^\top\Bigg]\cdot Q^\top\cdot \\
&\qquad \Bigg[-\dot{x}(t) + A_i x(t) + \sum_{m=1}^{M}\phi_{im}B_iK_m x(t-\tau(t))\Bigg]\Bigg\} \\
&\le \mathbb{E}\{\nu_1^\top(t)\Gamma_{1i}\nu_1(t)\}.
\end{aligned} \tag{3.20}$$

Since Eq (3.16) guarantees that $\Gamma_{1i} < 0$ for $i \in \{1,2,\ldots,N\}$, there exists a scalar $\sigma_1 > 0$ such that $\Gamma_{1i} \le -\sigma_1 I$, which implies $\nu_1^\top(t)\Gamma_{1i}\nu_1(t) \le -\sigma_1\|\nu_1(t)\|^2 \le -\sigma_1\|x(t)\|^2$. Therefore, it follows from Eq (3.20) that

$$\mathbb{E}\{\mathcal{L}V(x(t),t,r(t))\} \le -\sigma_1\mathbb{E}\left\{\|x(t)\|^2\right\}.$$

Part II: In the event-detection interval, i.e., $t \in [t_k + h, t_{k+1})$.

In this interval,

$$\begin{aligned}
\mathcal{L}V(x(t),t,r(t)) \le{}& 2x^\top(t)P_i\dot{x}(t) + x^\top(t)\Big(\sum_{j=1}^{N}\pi_{ij}P_j\Big)x(t) + x^\top(t)\delta t\,Rx(t) \\
&- \left(\frac{1}{\delta t}\int_{t-\delta t}^{t} x(s)\,\mathrm{d}s\right)^\top \delta t\,R\left(\frac{1}{\delta t}\int_{t-\delta t}^{t} x(s)\,\mathrm{d}s\right).
\end{aligned} \tag{3.21}$$

Adapting Eq (3.19) in Part I to the event-detection interval yields

$$0 = 2\Bigg[\dot{x}^\top(t) + x^\top(t) + \left(\frac{1}{\delta t}\int_{t-\delta t}^{t} x(s)\,\mathrm{d}s\right)^\top\Bigg]\cdot Q^\top\cdot\Bigg[-\dot{x}(t) + \left(A_i + \sum_{m=1}^{M}\phi_{im}B_iK_m\right)x(t) - \sum_{m=1}^{M}\phi_{im}B_iK_m e_k(t)\Bigg]. \tag{3.22}$$

During $t \in [t_k + h, t_{k+1})$, the triggering condition in the memory-based SETM in Eq (2.3) has not yet been satisfied, which implies

$$0 \le x^\top(t)\beta\Omega_i x(t) + \left(\frac{1}{\delta t}\int_{t-\delta t}^{t} x(s)\,\mathrm{d}s\right)^\top \beta\Omega_i\left(\frac{1}{\delta t}\int_{t-\delta t}^{t} x(s)\,\mathrm{d}s\right) - e_k^\top(t)\Omega_i e_k(t). \tag{3.23}$$

Let $\nu_2(t) = \operatorname{col}\left\{x(t), \dot{x}(t), e_k(t), \frac{1}{\delta t}\int_{t-\delta t}^{t} x(s)\,\mathrm{d}s\right\}$. Then, by combining Eqs (3.21)–(3.23), one obtains

$$\begin{aligned}
\mathbb{E}\{\mathcal{L}V(x(t),t,r(t))\} &\le \mathbb{E}\Bigg\{\mathcal{L}V(x(t),t,r(t)) + 2\Bigg[\dot{x}^\top(t) + x^\top(t) + \left(\frac{1}{\delta t}\int_{t-\delta t}^{t} x(s)\,\mathrm{d}s\right)^\top\Bigg]\cdot Q^\top\cdot \\
&\qquad \Bigg[-\dot{x}(t) + \Big(A_i + \sum_{m=1}^{M}\phi_{im}B_iK_m\Big)x(t) - \sum_{m=1}^{M}\phi_{im}B_iK_m e_k(t)\Bigg] \\
&\qquad + x^\top(t)\beta\Omega_i x(t) + \left(\frac{1}{\delta t}\int_{t-\delta t}^{t} x(s)\,\mathrm{d}s\right)^\top \beta\Omega_i\left(\frac{1}{\delta t}\int_{t-\delta t}^{t} x(s)\,\mathrm{d}s\right) - e_k^\top(t)\Omega_i e_k(t)\Bigg\} \\
&\le \mathbb{E}\{\nu_2^\top(t)\Gamma_{2i}\nu_2(t)\}.
\end{aligned} \tag{3.24}$$

Since Eq (3.17) guarantees that $\Gamma_{2i} < 0$ for $i \in \{1, 2, \ldots, N\}$, there exists a scalar $\sigma_2 > 0$ such that $\Gamma_{2i} \leq -\sigma_2 I$, which implies $v_2^\top(t)\Gamma_{2i}v_2(t) \leq -\sigma_2\|v_2(t)\|^2 \leq -\sigma_2\|x(t)\|^2$. Therefore, it follows from Eq (3.24) that

$$\mathbb{E}\{\mathcal{L}V(x(t), t, r(t))\} \leq -\sigma_2\mathbb{E}\Big\{\|x(t)\|^2\Big\}.$$

Part III: Synthesis.

This part proceeds along the same lines as the corresponding part of Theorem 1. Following Part III of Theorem 1, it can be concluded that the system in Eq (2.5) is stochastically stable under the memory-based SETM in Eq (2.3). The proof is complete.

Remark 4. By constructing different LKFs and employing free-weighting matrices, conditional expectation, Dynkin's formula, and several matrix inequalities, Theorems 1 and 3 establish two non-synchronous stochastic stability criteria. The former is applicable to the closed-loop system under the memoryless SETM in Eq (2.2), whose triggering condition depends only on the current state $x(t)$ and the measurement error $e_k(t)$. The latter applies to the closed-loop system under the memory-based SETM in Eq (2.3), in which the averaged historical state $\frac{1}{\delta t}\int_{t-\delta t}^{t} x(s)\,\mathrm{d}s$ is additionally incorporated into the triggering condition.

Remark 5. Non-synchronous ETM studies such as [32, 33] employ mode-dependent event-triggering rules, each governed by a single prescribed condition. Meanwhile, the SETMs in [19, 26] are formulated primarily in terms of instantaneous state or output information. By contrast, within a switched event-triggering structure and under the non-synchronous HMM framework, the memory-based SETM in Eq (2.3) considered in Theorem 3 incorporates the averaged historical state, thereby including recent state evolution in the triggering decision.

Theorem 4. *Given scalars $\beta > 0$ and $\delta t > 0$, if there exist matrices $\bar{P}_i > 0$, $\bar{\Omega}_i > 0$ $(i = 1, \ldots, N)$, $\bar{R} > 0$, $\bar{S} > 0$, an invertible matrix $\bar{Q}$, and general matrices $\bar{K}_m$ $(m = 1, \ldots, M)$ satisfying the following LMIs:*

$$\bar{\Gamma}_{1i} = \begin{bmatrix} \bar{\Xi}_{11}^{(1)} & \bar{\Xi}_{12}^{(1)} & \bar{\Xi}_{13}^{(1)} & \bar{\Xi}_{14}^{(1)} \\ * & -\mathrm{He}(\bar{Q}) & \bar{\Xi}_{23}^{(1)} & -\bar{Q}^\top \\ * & * & -\bar{S} & \bar{\Xi}_{34}^{(1)} \\ * & * & * & -\delta t\,\bar{R} \end{bmatrix} < 0, \tag{3.25}$$

$$\bar{\Gamma}_{2i} = \begin{bmatrix} \bar{\Xi}_{11}^{(2)} & \bar{\Xi}_{12}^{(2)} & \bar{\Xi}_{13}^{(2)} & \bar{\Xi}_{14}^{(2)} \\ * & -\mathrm{He}(\bar{Q}) & \bar{\Xi}_{23}^{(2)} & -\bar{Q}^\top \\ * & * & -\bar{\Omega}_i & \bar{\Xi}_{34}^{(2)} \\ * & * & * & \beta\bar{\Omega}_i - \delta t\,\bar{R} \end{bmatrix} < 0, \tag{3.26}$$

where

$$\bar{\Xi}_{11}^{(1)} = \delta t\,\bar{R} + \mathrm{He}(A_i\bar{Q}) + \sum_{j=1}^{N}\pi_{ij}\bar{P}_j,$$

$$\bar{\Xi}_{12}^{(1)} = \bar{P}_i - \bar{Q} + \bar{Q}^\top A_i^\top,$$

$$\bar{\Xi}_{13}^{(1)} = B_i\sum_{m=1}^{M}\phi_{im}\bar{K}_m,$$

$$
\begin{aligned}
\bar{\Xi}_{14}^{(1)} &= \bar{Q}^\top A_i^\top,\\
\bar{\Xi}_{23}^{(1)} &= B_i \sum_{m=1}^{M} \phi_{im} \bar{K}_m,\\
\bar{\Xi}_{34}^{(1)} &= \left(\sum_{m=1}^{M} \phi_{im} \bar{K}_m\right)^\top B_i^\top,\\
\bar{\Xi}_{11}^{(2)} &= \delta t \bar{R} + \beta \bar{\Omega}_i + \mathrm{He}(A_i \bar{Q}) + \mathrm{He}\left(B_i \sum_{m=1}^{M} \phi_{im} \bar{K}_m\right) + \sum_{j=1}^{N} \pi_{ij} \bar{P}_j,\\
\bar{\Xi}_{12}^{(2)} &= \bar{P}_i - \bar{Q} + \bar{Q}^\top A_i^\top + \left(\sum_{m=1}^{M} \phi_{im} \bar{K}_m\right)^\top B_i^\top,\\
\bar{\Xi}_{13}^{(2)} &= -B_i \sum_{m=1}^{M} \phi_{im} \bar{K}_m,\\
\bar{\Xi}_{14}^{(2)} &= \bar{Q}^\top A_i^\top + \left(\sum_{m=1}^{M} \phi_{im} \bar{K}_m\right)^\top B_i^\top,\\
\bar{\Xi}_{23}^{(2)} &= -B_i \sum_{m=1}^{M} \phi_{im} \bar{K}_m,\\
\bar{\Xi}_{34}^{(2)} &= -\left(\sum_{m=1}^{M} \phi_{im} \bar{K}_m\right)^\top B_i^\top,
\end{aligned}
$$

then the state-feedback controller in Eq (2.4) *with gain*

$$K_m = \bar{K}_m \bar{Q}^{-1},\ m \in \mathcal{M}$$

is able to achieve non-synchronous stabilization of the system in Eq (2.5)*.*

Proof. Set

$$P_i = (\bar{Q}^{-1})^\top \bar{P}_i \bar{Q}^{-1}, \quad \Omega_i = (\bar{Q}^{-1})^\top \bar{\Omega}_i \bar{Q}^{-1}, \quad R = (\bar{Q}^{-1})^\top \bar{R} \bar{Q}^{-1}, \quad S = (\bar{Q}^{-1})^\top \bar{S} \bar{Q}^{-1}, \quad Q = \bar{Q}^{-1},$$

and define

$$\mathcal{T} = \mathrm{diag}\left\{(\bar{Q}^{-1})^\top, (\bar{Q}^{-1})^\top, (\bar{Q}^{-1})^\top, (\bar{Q}^{-1})^\top\right\}.$$

Then, applying the transformation $\mathcal{T}(\cdot)\mathcal{T}^\top$ to the two inequalities $\bar{\Gamma}_{1i} < 0$ and $\bar{\Gamma}_{2i} < 0$, namely Eqs (3.25) and (3.26), gives

$$\mathcal{T}\bar{\Gamma}_{1i}\mathcal{T}^\top < 0,\ \mathcal{T}\bar{\Gamma}_{2i}\mathcal{T}^\top < 0.$$

By this congruence transformation, the inequalities (3.16) and (3.17) are obtained. Therefore, the feasibility of Eqs (3.25) and (3.26) implies the feasibility of Eqs (3.16) and (3.17). Thus, the proof is complete.

Remark 6. Theorem 2 provides a controller design scheme under the memoryless SETM in Eq (2.2). This scheme involves fewer decision variables, and its computational cost is lower. As shown in the numerical example below, the memoryless scheme in Theorem 2 can effectively reduce the number of triggering events. Theorem 4 provides a controller design scheme under the memory-based SETM in Eq (2.3). Compared with the triggering condition in Eq (2.2), the triggering condition in Eq (2.3) contains an additional memory term, which makes the corresponding LMI conditions more complicated. As a result, the scheme in Theorem 4 involves more decision variables and leads to a higher computational cost. As illustrated by the numerical example below, the memory-based scheme in Theorem 4 can further reduce the number of triggering events.

4. Numerical example

In this section, a multiple-mode vertical take-off and landing (VTOL) helicopter model, first studied in [34], is considered to illustrate the effectiveness of the proposed event-triggered control methods. Consistent with the system in Eq (2.1), the longitudinal dynamics of the helicopter are described by

$$\dot{x}(t) = A(\theta_t)x(t) + B(\theta_t)u(t),$$

where $A(\theta_t)$ is the (4×4) system matrix, $B(\theta_t)$ is the (4×2) input matrix, $x(t)$ is the 4-dimensional aircraft state vector, and $u(t)$ is the 2-dimensional input vector. Figure 1 shows the schematic diagram of the VTOL helicopter model, where the state variables are defined as follows: $x_1(t)$–horizontal velocity, $x_2(t)$–vertical velocity, $x_3(t)$–pitch rate, and $x_4(t)$–pitch angle.

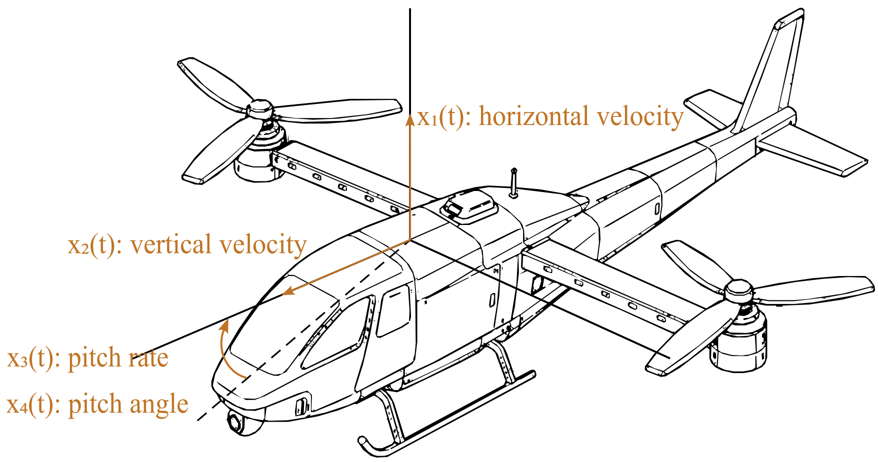

Figure 1. The VTOL helicopter model.

The mode-dependent matrices of the considered VTOL helicopter model are given by

$$A(\theta_t) = \begin{bmatrix} -0.0366 & 0.0271 & 0.0188 & -0.4555 \\ 0.0482 & -1.0100 & 0.0024 & -4.0208 \\ 0.1002 & a_{32}(\theta_t) & -0.7070 & a_{34}(\theta_t) \\ 0 & 0 & 1 & 0 \end{bmatrix},$$

$$B(\theta_t) = \begin{bmatrix} 0.4422 & 0.1761 \\ b_{21}(\theta_t) & -7.5922 \\ -5.5200 & 4.4900 \\ 0 & 0 \end{bmatrix}.$$

In this numerical example, the system mode $r(t)$ of the system in Eq (2.1) is denoted by θ_t. The behavior of θ_t is modeled as a Markov chain with three operating states corresponding to airspeeds of 135 (nominal value), 60, and 170 knots. The associated values of the parameters a_{32}, a_{34}, and b_{21} are listed in Table 1.

Table 1. Parameters corresponding to different airspeeds.

Airspeed (knots)	a_{32}	a_{34}	b_{21}
135	0.3681	1.4200	3.5446
60	0.0664	0.1198	0.9775
170	0.5047	2.5460	5.1120

The initial distribution of θ_t is taken as (0.6, 0.3, 0.1). The system mode transition is governed by the following transition rate matrix:

$$\Pi = \begin{bmatrix} -0.0171 & 0.0007 & 0.0164 \\ 0.0013 & -0.0013 & 0 \\ 0.0986 & 0 & -0.0986 \end{bmatrix}.$$

The controller mode is characterized by the following conditional probability matrix:

$$\Phi = \begin{bmatrix} 0.2193 & 0.7807 \\ 0.4130 & 0.5870 \\ 0.9766 & 0.0234 \end{bmatrix}.$$

For the memoryless scheme, the initial conditions of the system in Eq (2.1) are given by $x(0) = [0.05\ \ -0.05\ 0.1\ \ -0.1]^\top$. For the memory-based scheme, in order to make the memory term well defined on $t \in [0, \delta t]$, the interval $[-\delta t, 0]$ is taken as the prescribed initial history of the system. Accordingly, we set the initial conditions of the system in Eq (2.1) as $x(t) = [0.05\ \ -0.05\ 0.1\ \ -0.1]^\top$, $t \in [-\delta t, 0]$. The parameters are selected as $h = 0.3$, $\beta = 0.4$, and $\delta t = 0.3$. Figure 2 illustrates the response of $x(t)$ when no control input is applied, showing that the open-loop dynamics diverge. Figure 3 presents one possible evolution of the system mode $r(t)$ and controller mode $s(t)$.

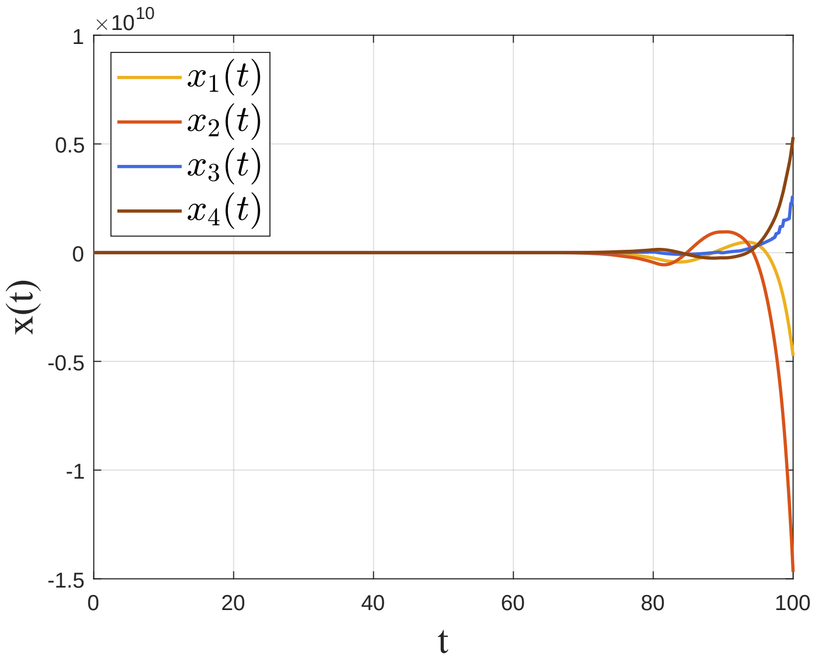

Figure 2. State trajectories without control input $u(t)$.

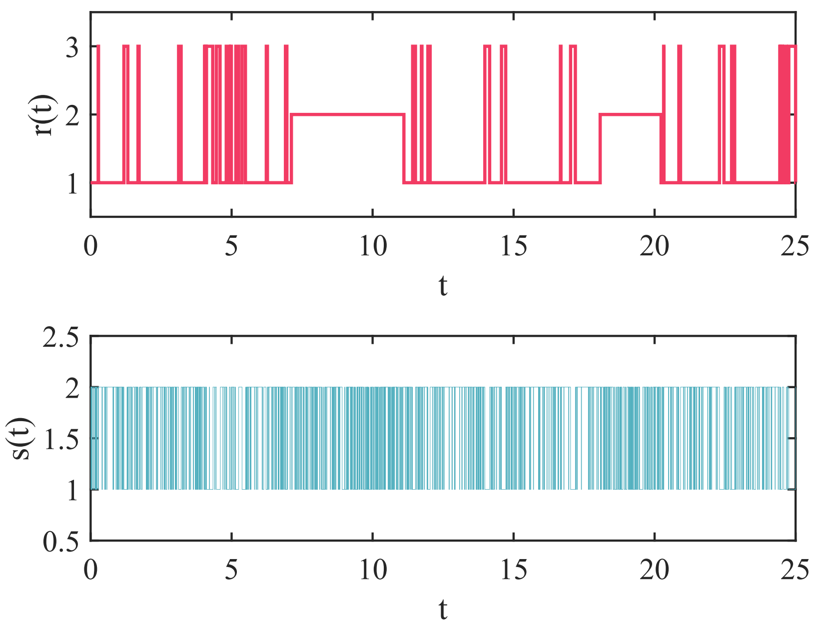

Figure 3. Switching processes of system modes and controller modes.

For the proposed memoryless scheme, by using the SeDuMi solver with the YALMIP interface to solve the LMI conditions in Theorem 2, we obtain the following control gains K_m:

$$K_1 = \begin{bmatrix} 0.5346 & 0.8368 & 1.2701 & 3.4989 \\ 0.9379 & 0.9536 & 0.7656 & 2.8654 \end{bmatrix},$$

$$K_2 = \begin{bmatrix} 0.2524 & 0.3712 & 0.8697 & 1.5543 \\ 0.4911 & 0.4813 & 0.5808 & 1.4307 \end{bmatrix}.$$

The corresponding state trajectories and inter-event intervals are shown in Figures 4 and 5, respectively.

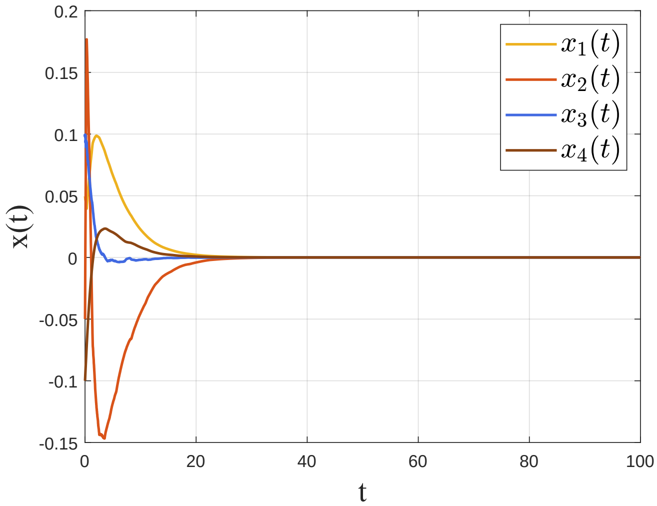

Figure 4. State trajectories under the memoryless SETM in Eq (2.2).

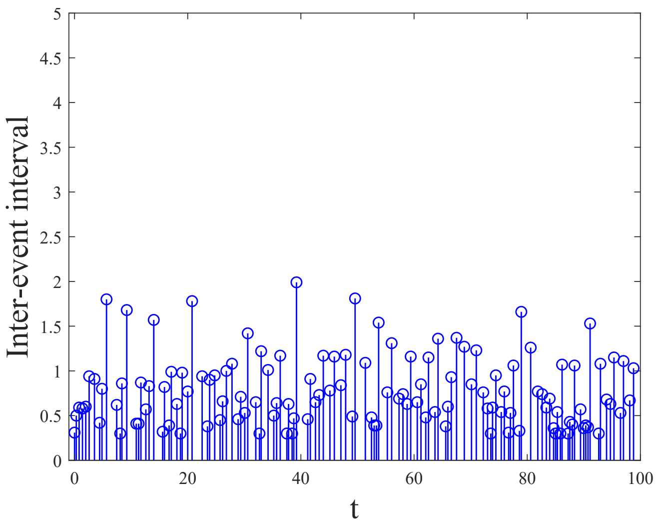

Figure 5. Inter-event intervals under the memoryless SETM in Eq (2.2).

It can be observed that all the state variables converge to zero, which verifies the effectiveness of the memoryless SETM.

For the proposed memory-based scheme, by using the SeDuMi solver with the YALMIP interface to solve the LMI conditions in Theorem 4, we obtain the following control gains K_m:

$$K_1 = \begin{bmatrix} -0.1153 & 0.1594 & 0.4493 & 1.4035 \\ -0.0075 & 0.0774 & 0.1923 & 0.4777 \end{bmatrix},$$

$$K_2 = \begin{bmatrix} -0.0344 & 0.0271 & 0.1863 & 0.2631 \\ 0.0593 & -0.0275 & -0.0733 & -0.4339 \end{bmatrix}.$$

The corresponding state trajectories and inter-event intervals are shown in Figures 6 and 7, respectively. It can be seen from the plot of inter-event intervals that the memory-based SETM generates significantly fewer triggering events.

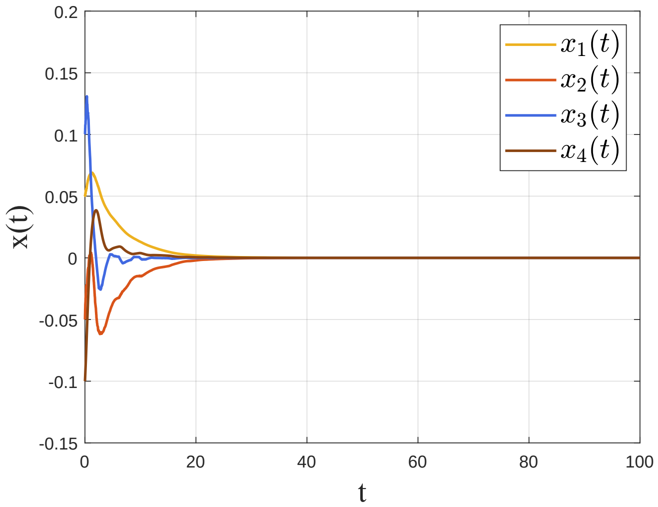

Figure 6. State trajectories under the memory-based SETM in Eq (2.3).

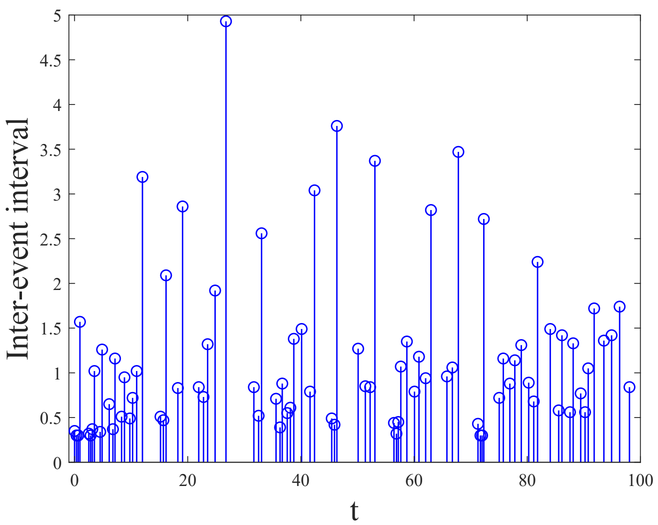

Figure 7. Inter-event intervals under the memory-based SETM in Eq (2.3).

To further demonstrate the effectiveness of the two proposed SETMs in reducing the controller update frequency, we additionally introduce Theorem 1 of [23] and Theorem 1 of [24] as baseline schemes. The ETMs adopted in these two references are different from those proposed in this paper. Specifically, reference [23] employs an adaptive ETM with an adjustable triggering threshold, and reference [24] adopts a mode-dependent ETM whose triggering condition varies with the transmitted data. Since neither of these two ETMs switches between the waiting interval and the event-detection interval, they provide meaningful benchmarks for evaluating the triggering performance of the proposed SETMs.

Building on the parameter setting introduced above, Table 2 compares the number of triggering events produced by the four triggering schemes as the triggering threshold β varies from 0.1 to 0.5, while the remaining parameters are kept unchanged. For every tested threshold, the memoryless scheme requires fewer triggering events than both methods in Theorem 1 of [23] and Theorem 1 of [24]. Therefore, the memoryless SETM can reduce the controller update frequency over the tested range of β. Furthermore, the memory-based scheme produces far fewer triggering events than the other three schemes at each threshold, confirming the additional reduction achieved by incorporating averaged historical state information into the triggering condition.

Table 2. Number of triggering events under different triggering schemes.

Triggering scheme	Number of triggering events for different β				
	$\beta = 0.1$	$\beta = 0.2$	$\beta = 0.3$	$\beta = 0.4$	$\beta = 0.5$
Theorem 1 of [23]	213	180	169	155	152
Theorem 1 of [24]	211	172	154	144	136
Memoryless scheme (Theorem 2)	191	148	129	129	116
Memory-based scheme (Theorem 4)	95	79	81	86	82

Table 3. Number of triggering events of the memory-based scheme for different h and δt.

h	Number of triggering events				
	$\delta t = 0.1$	$\delta t = 0.2$	$\delta t = 0.3$	$\delta t = 0.4$	$\delta t = 0.5$
0.1	91	80	81	91	88
0.2	94	85	94	81	88
0.3	82	78	81	83	84
0.4	82	82	78	81	73
0.5	76	81	84	76	69

Table 3 presents the number of triggering events of the memory-based scheme for different combinations of h and δt, with the triggering threshold set to $\beta = 0.3$ for this analysis. Across the ranges from 0.1 to 0.5 for both h and δt, the total number of triggering events does not exhibit a monotonically increasing or decreasing trend, but varies between 69 and 94. Compared with the other three triggering schemes reported in Table 2, the memory-based scheme consistently maintains fewer triggering events as h and δt vary, thereby achieving higher communication efficiency. Furthermore, among all the parameter combinations listed in Table 3, the combination $h = 0.5$ and $\delta t = 0.5$ achieves the highest communication efficiency in terms of triggering frequency, with the minimum number of triggering events being 69.

5. Conclusions

The stochastic stabilization problem for MJSs has been investigated under both memoryless and memory-based SETMs. For the memoryless SETM, Theorems 1 and 2 have provided the corresponding stochastic stability and controller design conditions in an LMI framework. For the memory-based SETM, by constructing an additional LKF, introducing more involved free-weighting matrix equalities that capture richer coupling relations, and employing matrix inequalities, stochastic stability and controller design conditions have been established in Theorems 3 and 4. Finally, a numerical example has demonstrated the ability of the proposed switched event-triggered non-synchronous state-feedback control schemes to achieve stochastic stability, and has further verified that both schemes can reduce the frequency of controller updates, with the memory-based scheme yielding fewer triggering events. The effects of β, h, and δt on the triggering performance have also been examined.

Use of AI tools declaration

The author declares he has not used Artificial Intelligence (AI) tools in the creation of this article.

Acknowledgments

This work was supported by the Undergraduate Innovation and Entrepreneurship Training Program of Anhui University of Technology (Grant No. S202510360214).

Conflict of interest

The author declares there is no conflict of interest.

References

1. C. Gong, G. Zhu, P. Shi, R. K. Agarwal, Distributed fault detection and control for Markov jump systems over sensor networks with round-robin protocol, *IEEE Trans. Circuits Syst. I Regul. Pap.*, **68** (2021), 3422–3435. https://doi.org/10.1109/TCSI.2021.3084969
2. R. Sakthivel, O. M. Kwon, S. G. Choi, R. Sakthivel, Observer-based state estimation for discrete-time semi-Markovian jump neural networks with round-robin protocol against cyber attacks, *Neural Netw.*, **165** (2023), 611–624. https://doi.org/10.1016/j.neunet.2023.05.046
3. Q. Wang, F. Zhu, L. Peng, Robust H_∞ filtering for semi-Markov jump systems encountering denial-of-service jamming attacks, *Circuits Syst. Signal Process.*, **41** (2022), 1453–1474. https://doi.org/10.1007/s00034-021-01853-z
4. J. Zhou, J. Dong, S. Xu, C. K. Ahn, Input-to-state stabilization for Markov jump systems with dynamic quantization and multimode injection attacks, *IEEE Trans. Syst. Man Cybern. Syst.*, **54** (2024), 2517–2529. https://doi.org/10.1109/TSMC.2023.3344869

5. N. Aravinth, T. Satheesh, R. Sakthivel, O. M. Kwon, Disturbance compensation-oriented security control for delayed singular switched semi-Markovian jump systems with hybrid cyber-attacks, *Int. J. Robust Nonlinear Control*, **36** (2026), 1461–1476. https://doi.org/10.1002/rnc.70201

6. J. Dhandapani, A. Neelamegam, V. Rajarathinam, M. Fazly, N. Gunasekaran, Robust H_∞ sampled-data sliding mode control for Markov switching stochastic neutral-type systems with mixed delays and Lévy noises, *Evol. Equ. Control Theory*, **21** (2026), 49–74. https://doi.org/10.3934/eect.2026034

7. Y. Y. Tao, Z. G. Wu, Asynchronous stabilization for hidden Markov jump linear systems with complex transition probabilities, *Automatica*, **156** (2023), 111200. https://doi.org/10.1016/j.automatica.2023.111200

8. J. Zhou, J. Dong, S. Xu, Asynchronous dissipative control of discrete-time fuzzy Markov jump systems with dynamic state and input quantization, *IEEE Trans. Fuzzy Syst.*, **31** (2023), 3906–3920. https://doi.org/10.1109/TFUZZ.2023.3271348

9. B. Wang, Q. Zhu, S. Li, Stabilization of hidden Markov jump singular systems with limit mode switching information, *IEEE Trans. Autom. Control*, **70** (2025), 3410–3416. https://doi.org/10.1109/TAC.2024.3518418

10. Q. Song, Q. Wu, Y. Liu, Stabilization of chaotic quaternion-valued neutral-type neural networks via sampled-data control with two-sided looped functional approach, *Nonlinear Anal. Model. Control*, **29** (2024), 1150–1166. https://doi.org/10.15388/namc.2024.29.37852

11. X. Chen, T. Jia, Z. Wang, X. Xie, J. Qiu, Practical fixed-time bipartite synchronization of uncertain coupled neural networks subject to deception attacks via dual-channel event-triggered control, *IEEE Trans. Cybern.*, **54** (2024), 3615–3625. https://doi.org/10.1109/TCYB.2023.3338165

12. Y. Yang, X. Zhu, L. Feng, L. Du, Prescribed-time stabilization for nonlinear systems via hybrid continuous and dynamic event-triggered impulsive control, *Networks Heterog. Media*, **20** (2025), 1251–1268. https://doi.org/10.3934/nhm.2025054

13. J. Ma, X. Chen, G. Wen, J. Wang, F. Zhao, J. Qiu, Dynamic memory event-triggered lag consensus of multi-UAV systems with hybrid attacks over stochastic switching topology, *IEEE Trans. Autom. Sci. Eng.*, **22** (2025), 16999–17009. https://doi.org/10.1109/TASE.2025.3580147

14. Z. Ming, H. Zhang, S. Yu, J. Ma, Self-triggered optimal control for unknown nonlinear random power systems with Markovian switching, *IEEE Trans. Syst. Man Cybern. Syst.*, **55** (2025), 1647–1656. https://doi.org/10.1109/TSMC.2024.3510594

15. S. Luo, X. Li, Y. Jiang, F. Deng, Stability, L_2-gain, and H_∞ control of linear Markov jump systems with periodic event-triggered sampling in state and mode, *Int. J. Robust Nonlinear Control*, **36** (2026), 993–1006. https://doi.org/10.1002/rnc.70167

16. Y. Chen, D. Zhang, X. Li, Two-channel dynamic event-triggered H_∞ control for Markovian jump systems under multiple cyber-attacks, *Trans. Inst. Meas. Control*, **47** (2025), 2127–2138. https://doi.org/10.1177/01423312241266688

17. L. Liu, J. Zhang, Y. Wang, P. Zhao, Dual-event-triggered sliding mode control for Markov jump systems with mismatched disturbances via a disturbance observer, *Eur. J. Control*, **89** (2026), 101505. https://doi.org/10.1016/j.ejcon.2026.101505

18. W. Wu, L. He, Z. Yan, J. Zhou, Event-triggered extended dissipativity stabilization of semi-Markov switching systems, *Appl. Math. Model.*, **118** (2023), 618–640. https://doi.org/10.1016/j.apm.2023.01.045

19. H. Wang, X. Hu, Z. Yan, Y. Chen, Event-driven stabilization for Markov jump systems based on disturbance observer, *IAENG Int. J. Comput. Sci.*, **52** (2025), 1378–1384, Available from: https://www.iaeng.org/IJCS/issues_v52/issue_5/IJCS_52_5_07.pdf.

20. Z. Yan, X. Huang, Y. Fan, J. Xia, H. Shen, Threshold-function-dependent quasi-synchronization of delayed memristive neural networks via hybrid event-triggered control, *IEEE Trans. Syst. Man Cybern. Syst.*, **51** (2021), 6712–6722. https://doi.org/10.1109/TSMC.2020.2964605

21. J. Zhou, D. Xu, W. Tai, C. K. Ahn, Switched event-triggered H_∞ security control for networked systems vulnerable to aperiodic DoS attacks, *IEEE Trans. Netw. Sci. Eng.*, **10** (2023), 2109–2123. https://doi.org/10.1109/TNSE.2023.3243095

22. Z. Wang, L. Yan, Y. Fan, F. Wang, H. Shen, Switching event-triggered-based gain-scheduled control for bipartite synchronization of coupled coopetitive memristive neural networks, *IEEE Trans. Syst. Man Cybern. Syst.*, **55** (2025), 6951–6963. https://doi.org/10.1109/TSMC.2025.3594542

23. D. Wen, X. Mu, Memory-based adaptive event-triggered asynchronous tracking control for semi-Markov jump systems with hybrid actuator faults, *Nonlinear Anal. Hybrid Syst.*, **49** (2023), 101359. https://doi.org/10.1016/j.nahs.2023.101359

24. L. Xie, J. Cheng, H. Wang, J. Wang, M. Hu, Z. Zhou, Memory-based event-triggered asynchronous control for semi-Markov switching systems, *Appl. Math. Comput.*, **415** (2022), 126694. https://doi.org/10.1016/j.amc.2021.126694

25. R. Suresh, G. Devi, R. Vadivel, N. Gunasekaran, L_1-gain stability analysis for Markov jump sampled-data control systems via co-positive-type LKF approach, *Int. J. Dyn. Control*, **14** (2026), 63. https://doi.org/10.1007/s40435-025-02000-1

26. A. Selivanov, E. Fridman, Event-triggered H_∞ control: A switching approach, *IEEE Trans. Autom. Control*, **61** (2016), 3221–3226. https://doi.org/10.1109/TAC.2015.2508286

27. B. Wang, Q. Zhu, The stabilization problem for a class of discrete-time semi-Markov jump singular systems, *Automatica*, **171** (2025), 111960. https://doi.org/10.1016/j.automatica.2024.111960

28. J. Zhao, N. Wu, X. Zhou, Reachable set bounding for delayed memristive neural networks via adaptive control, *Networks Heterog. Media*, **21** (2026), 198–212. https://doi.org/10.3934/nhm.2026009

29. Y. Y. Cao, J. Lam, Robust H_∞ control of uncertain Markovian jump systems with time-delay, *IEEE Trans. Autom. Control*, **45** (2000), 77–83. https://doi.org/10.1109/9.827358

30. X. Feng, K. A. Loparo, Y. Ji, H. J. Chizeck, Stochastic stability properties of jump linear systems, *IEEE Trans. Autom. Control*, **37** (1992), 38–53. https://doi.org/10.1109/9.109637

31. K. Gu, An integral inequality in the stability problem of time-delay systems, in *Proceedings of the 39th IEEE Conference on Decision and Control*, Sydney, NSW, Australia, **3** (2000), 2805–2810. https://doi.org/10.1109/CDC.2000.914233

32. J. Tao, Z. Xiao, J. Chen, M. Lin, R. Lu, P. Shi, et al., Event-triggered control for Markov jump systems subject to mismatched modes and strict dissipativity, *IEEE Trans. Cybern.*, **53** (2023), 1537–1546. https://doi.org/10.1109/TCYB.2021.3105179
33. Z. Xu, Y. Yu, Z. G. Wu, Y. Shen, Asynchronous event-triggered H_∞ control for continuous-time Markov jump systems, *IEEE Control Syst. Lett.*, **8** (2024), 3386–3391. https://doi.org/10.1109/LCSYS.2025.3534476
34. K. S. Narendra, S. S. Tripathi, Identification and optimization of aircraft dynamics, *J. Aircr.*, **10** (1973), 193–199. https://doi.org/10.2514/3.44364

AIMS Press